BMC Plant Biology

RESEARCH Open Access

Integrative transcriptomic and metabolomic profiling elucidates the metabolic network underlying development in *Salsola collina*

Ye Chen[1], Wenhui Bi[1], Jinyan Hao[1], Shipeng Li[2], Wenli Wu[1], Songdan Zheng[1], Mingxing Wang[1], Yanli Fan[1], Yongjie Ma[1] and Huiyuan Ya[1*]

Abstract

Background *Salsola collina* Pall. is a typical food-medicinal resource with considerable nutritional and medicinal value. However, systematic investigations into the dynamic changes in the chemical composition of the leaves of this species during the growth cycle remain limited to date.

Results An integrated approach of transcriptomics and metabolomics was employed to identify and analyze the metabolites and genes in *S. collina* leaves at different growth stages in this study. A total of 1,125 differentially accumulated metabolites (DAMs) and 16,200 differentially expressed genes (DEGs) were identified. Mapping of the DEGs and DAMs to Kyoto Encyclopedia of Genes and Genomes (KEGG) pathways revealed the significant enrichment of the phenylpropanoid biosynthesis pathway and flavonoid biosynthesis pathway, which were then considered core metabolic pathways. Within these two pathways, 258 DEGs and 26 DAMs were detected. The *C4H* and *4CL* genes were expressed at relatively high levels during flowering, and the expression levels of most *CHS*, *F3H*, *FLS*, and *ANR* genes were relatively high during fruiting. The total flavonoid, polyphenol, and alkaloid contents peaked at the flowering stage, with values of 8.944 mg/g, 6.659 mg/g, and 6.616 mg/g, respectively.

Conclusions This study elucidates the regulatory effect of growth stage on the secondary metabolites in *S. collina* leaves, providing a theoretical basis and experimental evidence to support the research aimed at determining the precise harvesting time and realizing the efficient utilization of *S. collina* resources.

Keywords *Salsola collina* Pall., Transcriptome, Metabolome, Flavonoid biosynthesis

*Correspondence:
Huiyuan Ya
yahuiyuan@lynu.edu.cn
[1]College of Food and Drug, Luoyang Normal University, Luoyang, Henan, China
[2]College of Life Science, Luoyang Normal University, Luoyang, Henan, China

Introduction

Salsola collina Pall. is a species belonging to the order Caryophyllales and family *Amaranthaceae*, and is widespread in Henan, Sichuan, Yunnan, Jiangsu, and other places in China [1, 2]. The whole herb *S. collina* is used as a medicine for treating hypertension, headache, insomnia, constipation, and dizziness in China [3].

S. collina has been utilized for culinary, pharmaceutical, and health purposes [1]. The extract of *S. collina* promotes intestinal peristalsis, reduces blood lipid levels, and improves gastric emptying; it also exerts a certain pharmacological effect that is useful in the treatment of diabetic gastroparesis [4–6]. *S. collina* reportedly possesses significant anti-aging activity, and a novel preparation derived from its components demonstrates dual senomorphic and senolytic activities. The preparation exerts specific anti-aging effects by regulating the p53-CDK2 signaling pathway, improves senescent phenotypes in both senescent cells and animal models, and extends healthy lifespan, all of which further support its potential as a natural resource for pharmacological interventions[7].

Various secondary metabolites have been identified from Salsola so far, including flavonoids, alkaloids, phenolic acids, fatty acids and their derivatives, and sterols [8–12]. Li et al. reported successful detection of 637 metabolites in the leaves and roots of *S. collina*. Among these metabolites, flavonoids accounted for 23.55% of the total composition, phenylpropanoids accounted for 18.05%, lipids 17.58%, amino acids 10.99%, and alkaloids 6.9%. Flavonoids, alkaloids, lignans, and coumarins are speculated to be the main bioactive components of Salsola [13].

The chemical composition and pharmacological activity of plants significantly differ at different developmental stages [14]. The accumulation of active materials in plants is influenced by various factors, including the plant growth process, degree of organ differentiation, and maturity [15, 16]. For example, the contents of active components in *Lonicera japonica* Thunb. peak at milky and early white bud stages [17]. The contents of polysaccharides and amino acids in the fruiting bodies of *Ganoderma lucidum* (Curtis) P. Karst were positively correlated with their growth stages, and the aqueous extract of fruiting bodies at the cyan mature stage exhibited the most significant hepatoprotective effect [18]. The blood pressure-regulating effect of *S. collina* varies with the growth stage [2]. Moreover, there is a lack of systematic research on the dynamic changes in the composition of active substances in *S. collina* during development.

In this study, metabolomics and transcriptomics technologies were employed to analyze and screen the DAMs and DEGs of the leaves of *S. collina* during development. Moreover, the differentially expressed genes related to the flavonoid synthesis pathway in *S. collina* and the candidate genes and metabolites that play key roles in the flavonoid biosynthesis pathway were identified. These results shed light on the metabolic pathways underlying development, providing novel ideas and a scientific basis for the application of *S. collina.*

Materials and methods

Plant materials

The wild individuals of *Salsola collina* Pall. were collected from Luoyang Normal University, Henan Province, China (N 34°37′43″, E 112°36′4″). The *S. collina* leaves samples, L-Sc1, L-Sc2 and L-Sc3, were collected at the juvenile stage (April 2023), flowering stage (July 2023), and fruiting stage (September 2023). Some of the samples was frozen in liquid nitrogen at − 80 °C to extract the RNA and the metabolites. The other samples was washed and then dried in oven at 37 °C for the determination of total flavonoid, phenol, and alkaloid contents. Furthermore, all the experiments were conducted in three biological samples to ensure reproducibility.

Metabolite profiling using UPLC-MS/MS

The freeze-dried samples were crushed using a mixer mill (MM 400, Retsch) and zirconia beads for 1.5 min at 30 Hz. One hundred milligrams of powder was weighed and extracted overnight at 4 °C in 1.0 mL of 70% aqueous methanol (v/v). Following centrifugation at 10,000 × g for 10 min, the extracts were filtered using a Millipore filtration system (ANPEL, Shanghai, China) before the LC-MS analysis. For each sample, three biological replicates were independently analyzed, and the UPLC-MS analysis was carried out using a 6500 triple quadrupole-linear ion trap mass spectrometer (AB Sciex, Framingham, USA) under the following conditions: HPLC column, Waters ACQUITY UPLC HSS T3 C18 (1.8 µm, 2.1 mm × 100 mm); solvent system, water (0.04% acetic acid): acetonitrile (0.04% acetic acid); gradient program, 95:5 V/V at 0 min, 5:95 V/V at 11.0 min, 5:95 V/V at 12.0 min, 95:5 V/V at 12.1 min, 95:5 V/V at 15.0 min; flow rate, 0.40 mL/min; temperature, 40 °C; injection volume, 2 µL. The sample was injected into the chromatographic column. Driven by the mobile phase, different compounds eluted from the column sequentially at different retention times. Afterwards, the effluent was introduced into an electrospray ionization (ESI) source for vaporization and then entered the triple quadrupole-linear ion trap (QTRAP)-MS an electrospray ionization (ESI)-triple Q-TRAP-MS.

The mass spectrometry analysis followed the methods of Chen et al. [19]. The ESI source operation parameters were as follows: ion source, turbo spray; source temperature, 500 °C; ion spray voltage (IS), 5500 V; ion source gas I (GSI), gas II (GSII), and curtain gas (CUR) set at 55, 60, and 25.0 psi, respectively; high collision gas (CAD).

Instrument tuning and mass calibration were performed using 10 and 100 μmol/L polypropylene glycol solutions in QQQ and LIT modes, respectively. The QQQ scans were acquired as multiple reaction monitoring (MRM) experiments, and the collision gas (nitrogen) pressure was set to 0.34 bar. Qualitative and quantitative analyses of the metabolites were conducted following the methods of Wang et al. [20]. Qualitative analysis of the primary and secondary MS data was carried out through the comparison of accurate precursor ion (Q1) and product ion (Q3) values and retention time (RT) values using the self-built database MWDB (MetWare Biotechnology Co. Ltd. Wuhan, China) and public metabolite databases, namely, MassBank (http://www.massbank.jp/), KNAPSAcK (http://kanaya.naist.jp/KNApSAcK/), HMDB (http://www.hmdb.ca/), MoToDB (http://www.ab.wur.nl/moto/), ChemBank (http://chembank.med.harvard.edu/compounds), PubChem (https://pubchemblog.ncbi.nlm.nih.gov/), NIST Chemistry Webbook (http://webbook.nist.gov/), and METLIN (http://metlin.scripps.edu/index.php). The quantitative analysis of metabolites was performed using MRM analysis and QQQ mass spectrometry. To monitor analytical drift and matrix effects, 2-chlorophenylalanine was added to the samples as an internal standard. In the MRM mode, the quadrupole filters the precursor ions of the target substance and excludes the ions corresponding to the other molecular weights to eliminate interference. After the metabolite MS data of the different samples are obtained, peak area integration is performed. Finally, the chromatographic peak area was used to determine the relative metabolite contents.

Metabolomic data analysis

The filtered data were submitted to Simca-P software (version 13.0, Umetrics AB, Umea, Sweden) to attain the results for unsupervised principal component analysis (PCA) and orthogonal partial least squares-discriminant analysis (OPLS-DA) [21]. Hierarchical clustering analysis of the metabolites between the samples was performed using R software (www.r-project.org). In order to identify the differentially accumulated metabolites (DAMs), the screening criteria of fold change ≥ 2 or ≤ 0.5 and variable importance in project (VIP) ≥ 1 were used.

RNA-seq analysis

The *S. collina* samples were extracted through ethanol precipitation and CTAB-PBIOZOL. Approximately 50–100 mg of ground *S. collina* leaves was lysed in 1 mL CTAB buffer supplemented with β-mercaptoethanol via gentle inversion. Following incubation at 65 °C (800 rpm, 10 min) in a thermomixer, homogenates were centrifuged at 12,000 × g for 5 min at 4 °C. Supernatants were extracted twice with an equal volume of chloroform/isoamyl alcohol (24:1, v/v), then mixed with an equal volume of LiCl solution and precipitated at − 20 °C for ≥ 2 h. After centrifugation at 12,000 × g for 20 min at 4 °C, pellets were washed with 75% ethanol, air-dried, and resuspended in 30 μL DEPC-treated water containing 1% DNase I. Following vortexing and incubation at 37 °C for 10 min, samples were briefly centrifuged and stored at − 80 °C until use [22]. A TruSeqTM RNA sample preparation kit (Illumina, United States) was used according to the manufacturer's instructions, and cDNA libraries were generated from the mRNA from each sample. Since there is no reference genome available for *S. collina*, clean reads were subjected to transcript assembly using Trinity, and the assembled transcripts were clustered and de-redundanded with Corset [23]. Fragments per kilobase million (FPKM) values were used to evaluate gene expression. Raw read counts were used to perform differential expression analysis across sample groups using DESeq2 [24]. The Benjamini-Hochberg method was applied to correct the *P* values obtained from hypothesis tests for multiple testing, thereby calculating the False Discovery Rate (FDR). The filter criterion was | log2(fold change) | > 1, with a FDR < 0.05. In order to further understand the functions and important pathways of the identified DEGs, TopGO and clusterProfiler were utilized for enriching all DEGs through Gene Ontology (GO) and the Kyoto Encyclopedia of Genes and Genomes (KEGG).

Quantitative real-time PCR (qRT-PCR) analysis

Total RNA was isolated using a Plant RNA Extraction Kit (Cat. No. 9769; TakaRa Biotechnology Inc., Shiga, Japan). The concentration of the extracted RNA was measured using a NanoDrop 2000 (ThermoFisher Scientific Inc., Waltham, USA). First-strand cDNA was synthesized from 1 μg of the total RNA by following the protocol provided with the PrimeScript™ RT reagent kit with gDNA Eraser (Cat. No. RR047A; TakaRa Biotechnology Inc., Shiga, Japan). The qRT-PCR analysis was carried out using the CFX96™ Real-Time System (Bio-Rad Laboratories, Inc., Hercules, USA). qRT-PCR was carried out in 25 μL reaction volumes (TakaRa, Cat. No. RR820A) with gene specific primers as directed by the manufacturer. The Bio-Rad CFX96 Real-Time PCR Detection System was employed to identify and monitor the generated amplification signals. The qPCR programme was initiated with a preliminary step of 95 °C for 35 s, followed by 40 cycles of 95 °C for 5 s, 60 °C for 30 s, and 72 °C for 10 s. Relative expression values were calculated using the $2^{-\Delta\Delta Ct}$ method [25]. The ACTIN gene (*Cluster-25127.76*) was used as the internal control [26]. All expression level data obtained through qRT-PCR were based on three biological samples and three replicates for each sample. The primers used for qRT-PCR are provided in Table S1.

Determination of bioactive substances

In this study, the contents of flavonoids, total phenols, and alkaloids were used to compare the bioactive substances L-Sc1, L-Sc2, and L-Sc3. The flavonoid content was determined using a Plant Flavonoid Content Assay Kit (BC1330, Solarbio Life Sciences) with visible spectrophotometry. The assay is based on the formation of a characteristic red complex between flavonoids and aluminum ions in an alkaline nitrite system, with absorbance detected at 470 nm. Each specimen, weighing about 0.1 g, was extracted with 1 mL of 60% ethanol under ultrasonic conditions (300 W, 60 °C) for 30 min. The mixture was then centrifuged at 12,000 rpm for 10 min. Subsequent to supernatant isolation, an aliquot comprising 0.2 mL of the sample was blended with 0.05 mL of 5% sodium nitrite ($NaNO_2$) and incubated for a duration of 5 min. After that, 0.05 mL of NaOH (4%) was poured after adding another 0.4 mL of 5% NaNO2, mixing, and incubating for a duration equal to 5 min. Following vortex mixing and incubation, the reaction mixture was incubated at 37 °C for 45 min, then centrifuged at 10,000 × g for 10 min. The blank was a reagent solution that contained distilled water. Total flavonoid concentrations were determined using a rutin standard curve and absorbance measurements at 470 nm [27].

$$\text{Plant flavonoid content} = \mathrm{C} \times \mathrm{V} \times \mathrm{N}/\mathrm{W} \quad (1)$$

where, C represents the concentration of the sample (mg/mL), V represents the extracted volume (mL), N represents the sample dilution factor, and W represents the sample mass.

Total phenolic content was determined using the Plant Total Phenol (TP) Assay Kit (BC1340, Solarbio, Beijing, China) with visible spectrophotometry. The method is based on the reduction of Folin-Ciocalteu reagent by phenolic compounds under alkaline conditions to generate a blue compound with characteristic absorption at 760 nm. Approximately 0.1 g of sample was extracted with 2.5 mL of 60% ethanol in an ultrasonic bath (300 W, 60 °C) for 30 min, followed by centrifugation at 12,000 rpm for 10 min. Gallic acid was used as the standard for calibration curve construction. Subsequent to supernatant isolation, 50 μL of supernatant was mixed with 250 μL of Folin–Ciocalteu reagent and incubated at room temperature for 2 min, then mixed with 250 μL of alkaline sodium carbonate solution and 450 μL of distilled water, and incubated for another 10 min. The blank was a reagent solution that contained distilled water, absorbance was measured at 760 nm.Total phenolic content was calculated as mg per gram dry weight using the standard curve [28].

$$\text{Total phenolic content} = \mathrm{C} \times \mathrm{V} \times \mathrm{N}/\mathrm{W} \quad (2)$$

where, C represents the concentration of the sample (mg/mL), V represents the extracted volume (mL), N represents the sample dilution factor, and W represents the sample mass.

Total alkaloid content was determined using an Alkaloid Assay Kit (BC6230, Solarbio Life Sciences, Beijing, China) with visible spectrophotometry. The method is based on the reaction of alkaloids with bromocresol green to form a yellow-green complex with characteristic absorption at 416 nm. Approximately 0.1 g of sample was extracted with 1 mL of extraction buffer at room temperature under ultrasonication for 60 min, followed by centrifugation at 8000 × g for 10 min, and the supernatant was collected for analysis. Briefly, 150 μL of sample supernatant, standard solution, extraction solution, methanol, was mixed with 300 μL of bromocresol green chromogenic reagent and 750 μL of auxiliary reagent, vortexed, and incubated at room temperature for 5 min. Then, 1500 μL of chloroform was added, mixed thoroughly, and left to stand for 40 min at room temperature. The lower chloroform layer was collected and measured at 416 nm. Berberine hydrochloride was used as a reference standard, and the results were expressed as berberine hydrochloride equivalents in mg/g extract [29].

$$\text{Total alkaloid content} = \mathrm{C} \times \mathrm{V} \times \mathrm{N}/\mathrm{W} \quad (3)$$

where, C represents the concentration of the sample (mg/mL), V represents the extracted volume (mL), N represents the sample dilution factor, and W represents the sample mass.

Statistical analysis

Statistical analyses were conducted using R software and IBM SPSS statistical software (https://www.ibm.com/analytics/spss-statistics software). The data were analyzed using one-way analysis of variance (ANOVA) and Pearson's correlation tests at the 5% significance level.

Results

Comparison of the concentrations of the principal chemical constituents of *S. collina* leaves during different stages

In order to investigate the dynamic changes in the bioactive components of *S. collina* leaves, flavonoids, polyphenols, and alkaloids were quantified at three developmental stages (Fig. 1). The results revealed differences in the flavonoid, polyphenol, and alkaloid contents of the *S. collina* leaves. As shown in Fig. 1A and B, the total flavonoids and total polyphenols increased from L-Sc1

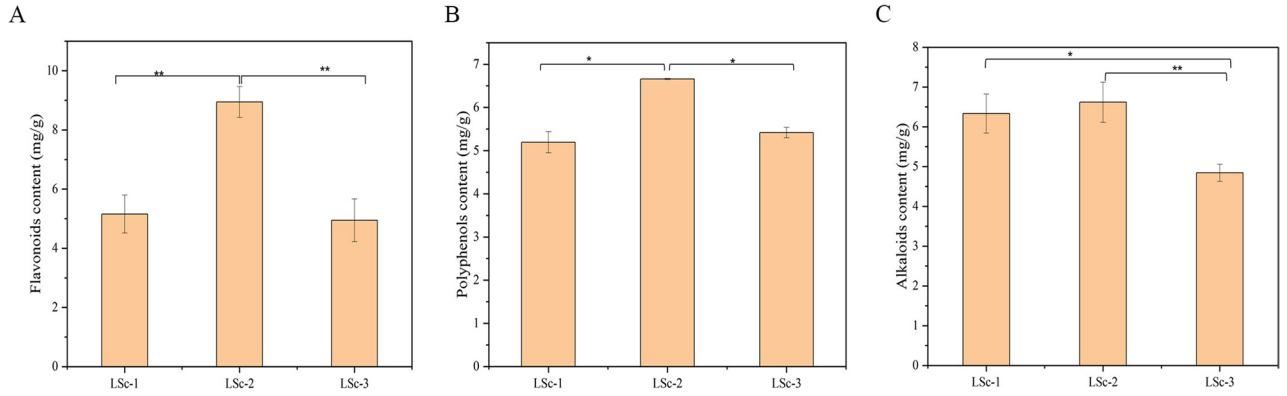

Fig. 1 Contents of the major chemical components in *Salsola collina*.**A** Content of total flavonoids. **B** Content of total polyphenols. **C** Contents of total alkaloids. *$p < 0.05$, significant difference; **$p < 0.01$, highly significant difference for the same index among different growth stages

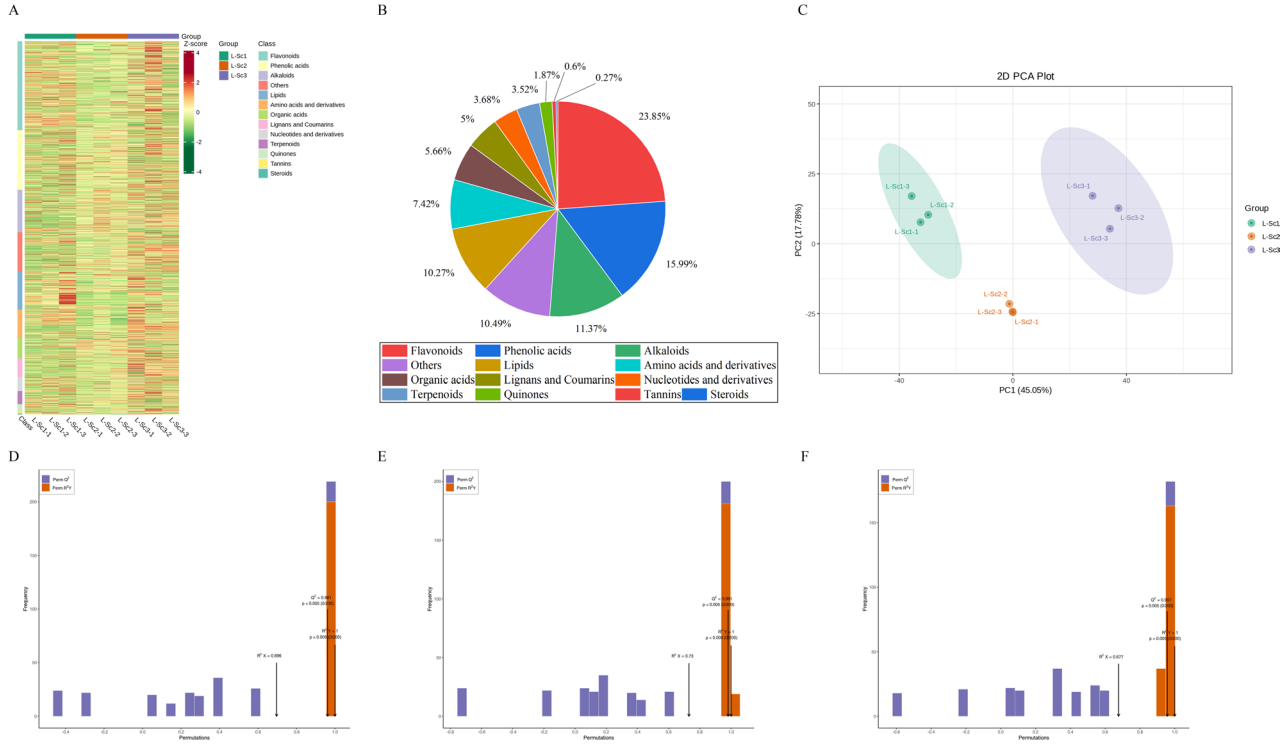

Fig. 2 Qualitative and quantitative analyses of the metabolomics data of *Salsola* leaves. **A** Heatmap of quantified metabolites. Color scale represents relative metabolite accumulation levels. **B** A ring chart depicting the number of different metabolite classes. **C** A scatter plot displaying PCA scores for all metabolites. OPLS-DA for (**D**) L-Sc1 vs. L-Sc2, (**E**) L-Sc1 vs. L-Sc3, and (**F**) L-Sc3 vs. L-Sc2

to L-Sc2, demonstrated a gradual decrease from L-Sc2 to L-Sc3, and the maximum values reached 8.944 mg/g and 6.659 mg/g, respectively, at the flowering stage(L-Sc2). Moreover, the alkaloid content of *S. collina* leaves was measured at different developmental stages (Fig. 1C). There was a slight increase in the alkaloid content from L-Sc1 to L-Sc2, a very significant decrease from L-Sc2 to L-Sc3, and the highest alkaloid content of 6.616 mg/g was found in the flowering stage(L-Sc2). These results indicated that the flowering stage is the optimal period for flavonoid, polyphenol, and alkaloid accumulation.

Metabolic profiling and changes between the different stages of *S. collina* leaf development through PCA and OPLS-DA

In order to evaluate the changes in the intracellular metabolism of *S. collina* leaves, dynamic profiling of the intracellular metabolites was performed using widely targeted metabolomics methods. The metabolites were quantitatively analyzed using software Analyst under the multiple reaction monitoring modes (Fig. S1). A total of 1,820 metabolites were identified in the *Salsola* leaves (Fig. 2A and Table S2). As shown in Fig. 2B, the

metabolites were identified and could be categorized into over 13 different classes, including 434 flavonoids (23.85%), 291 phenolic acids (15.99%), 207 alkaloids (11.37%), 187 lipids (10.27%), 135 amino acids and their derivatives (7.42%), 103 organic acids (5.66%), 91 lignans and coumarins (5.00%), 67 nucleotides and their derivatives (3.68%), 64 terpenoids (3.52%), 34 quinones (1.87%), 11 tannins (0.60%), five steroids (0.27%), and 191 others (10.49%).

In order to further analyze the degree of variability in the intergroup samples and intragroup samples, the metabolite profiles of 9 samples were subjected to PCA. The two principal components, PC1 and PC2, explained 45.04% and 16.56% of the total variability, respectively. In the PCA plot, the L-Sc1, L-Sc2, and L-Sc3 samples were clearly separated (Fig. 2C). The OPLS-DA score plot also revealed an obvious separation between the discriminant classes L-Sc1, L-Sc2, and L-Sc3 (Fig. 2D, E and F). High predictability (Q2) and strong goodness of fit (R2X, R2Y) were observed between L-Sc1 and L-Sc2 (Q2 = 0.961, R2X = 0.696, R2Y = 1; Fig. S2A), L-Sc1 and L-Sc3 (Q2 = 0.981, R2X = 0.73, R2Y = 1; Fig. S2B), and L-Sc3 and L-Sc2 (Q2 = 0.957, R2X = 0.677, R2Y = 1; Fig. S2C). The parameters indicated that these models were stable and reliable and could, therefore, be used to further identify the differentially abundant metabolites. Taken together, these results suggested that L-Sc1, L-Sc2, and L-Sc3 presented significantly distinct metabolic profiles.

Metabolomic variations among the different stages of *S. collina* leaf development

In order to dissect the metabolic variations among the different stages of *S. collina*, the metabolite profiles of L-Sc1, L-Sc2, and L-Sc3 were compared, and the significantly differentially abundant metabolites (DAMs) were selected. As presented in Fig. 3A and Table S3, a total of 1125 DAMs were identified, mainly including 252 flavonoids (22.4%), 212 phenolic acids (18.84%), 143 alkaloids (12.71%), and 107 lipids (9.51%). In order to analyze the DAM accumulation pattern, the metabolomics data were centralized and standardized, and then analyzed using K-means clustering. As shown in Fig. 3B and Table S4,

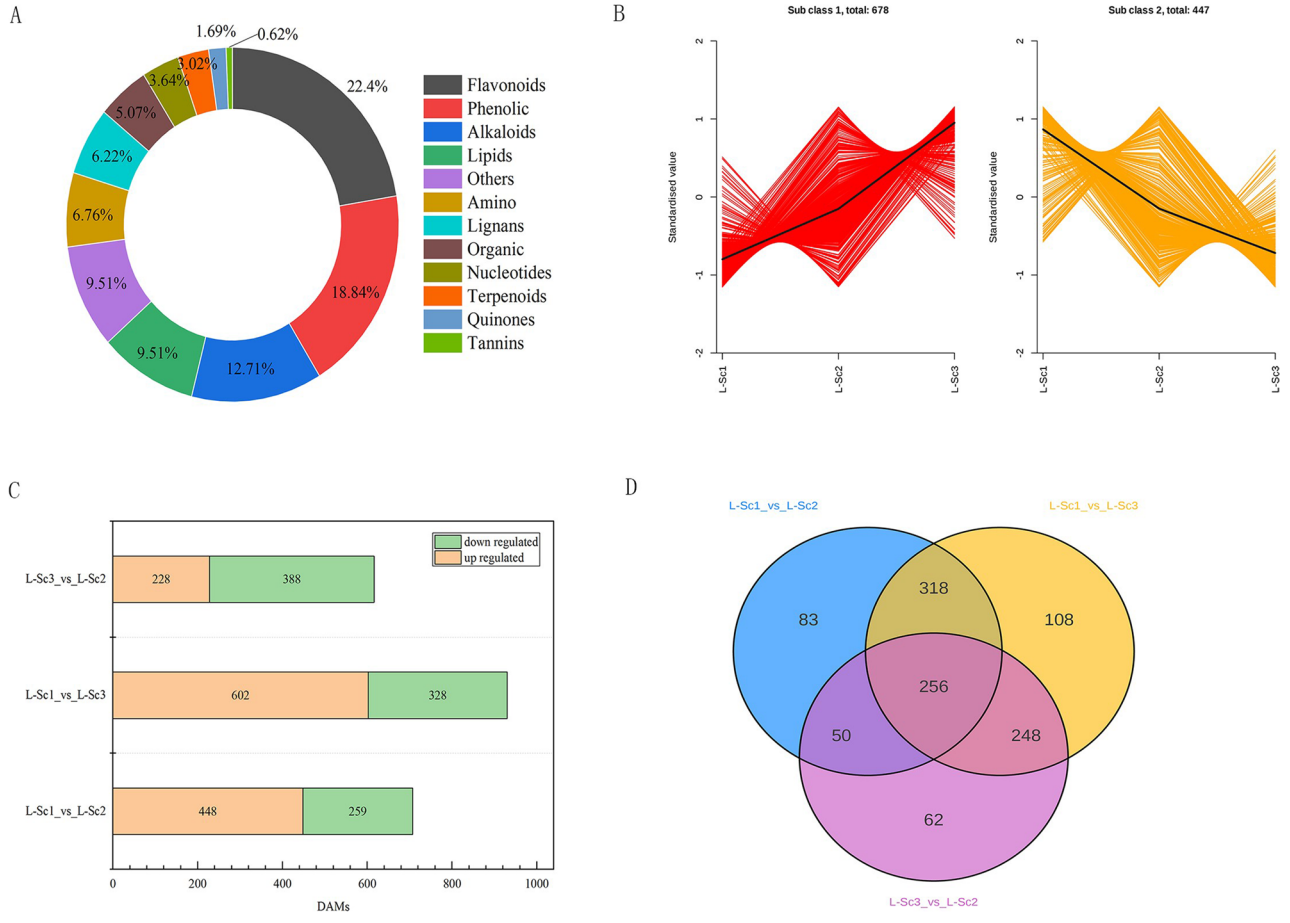

Fig. 3 (A) Component analysis of the identified metabolites in *Salsola*. **B** K-means clustering analysis of the DAM accumulation patterns in *Salsola*. **C** DAMs that were upregulated or downregulated in the different stages of *Salsola* leaf development. **D** Venn diagram showing the number of DAMs in L-Sc1, L-Sc2, and L-Sc3 groups

the DAMs were clustered into two subclasses. A total of 678 metabolites in subclass 1 gradually increased with leaf development. A total of 447 metabolites in subclass 2 presented the highest relative concentrations at the flowering stage.

Among the three *S. collina* leaf samples, 707, 930, and 616 DAMs were detected in L-Sc1 vs. L-Sc2, L-Sc1 vs. L-Sc3, and L-Sc3 vs. L-Sc2, respectively. Compared with those in L-Sc2, there were 259 upregulated metabolites and 448 downregulated metabolites in L-Sc1. Compared with those in L-Sc3, 328 and 602 metabolites were upregulated and downregulated in L-Sc1, respectively. Compared with those in L-Sc2, 388 and 228 metabolites were upregulated and downregulated in L-Sc3 (Fig. 3C and Table S5).

A Venn diagram was prepared to illustrate the common and unique metabolite changes between the different comparison groups, the data of which are summarized in Table S6. As shown in Fig. 3D, L-Sc1 vs. L-Sc2 and L-Sc1 vs. L-Sc3 had 318 DAMs, including dopamine, kakkalide, and laricitrin. A total of 83 unique metabolites, including flavonoids, lipids, amino acids, and their derivatives, were observed in L-Sc1 vs. L-Sc2. There were 50 metabolites common to L-Sc1 vs. L-Sc2 and L-Sc3 vs. L-Sc2, and 62 unique metabolites were found in L-Sc3 vs. L-Sc2. 248 common metabolites were observed between L-Sc1 and L-Sc3 and between L-Sc3 and L-Sc2, and 108 unique metabolites were found between L-Sc3 and L-Sc2. L-Sc1 vs. L-Sc2, L-Sc1 vs. L-Sc3, and L-Sc3 vs. L-Sc2 shared 256 metabolites with common changes. These substances were mainly flavonoids, phenolic acids, and alkaloids, which play critical roles in the growth and development of Salsola. Accordingly, these key metabolites, including flavonoids, phenolic acids, and alkaloids, were selected for further investigation.

In this study, a total of 252 differential flavonoids were identified, encompassing 10 categories that included flavones, flavonols, and dihydroflavones. The heatmap depicted in Fig. 4A shows 70 common differential flavonoids, such as chrysin, hesperetin, homoeriodictyol, and naringenin (5,7,4'-trihydroxyflavanone); 32 unique flavonoids were detected in the L-Sc1 vs. L-Sc2 comparison group, including cirsilineol (4',5-dihydroxy-3',6,7-trimethoxyflavone) and rutin trihydrate. In the L-Sc1 vs. L-Sc3 comparison group, 26 unique flavonoids were identified, with the representatives including phloretin-2'-O-glucoside (phlorizin) and epicatechin, among the 13 types. Additionally, 15 unique flavonoids, such as acacetin and kaempferol (3,5,7,4'-tetrahydroxyflavone), were found in the L-Sc3 vs. L-Sc2 group. In this study, the contents of most flavonoids tended to increase during the growth and development process. Specifically, 6,4'-dimethoxyisoflavone-7-O-glucoside (wistin), afrormosin rutinoside, and 4'-demethyleucomin glucosyl rhamnoside reached their maximum levels in the L-Sc3 stage.

Two hundred twelve differential phenolic acids were identified. The expression profiles of 44 phenolic acids, such as arbutin, 4-caffeoylshikimic acid, coniferin, dihydroferulic acid, and gastrodin, were significantly different (Fig. 4B). Nine unique phenolic acids were detected in the L-Sc1 vs. L-Sc2 comparison group, including 3-O-feruloylquinic acid-O-glucoside, chlorogenic acid methyl ester, and orobanchoside. In the L-Sc1 vs. L-Sc3 group, 26 unique phenolic acids were identified, including 1-caffeoylquinic acid, ferulic acid, and salidroside. Additionally, 12 unique phenolic acids, such as 3-O-caffeoylquinic acid, coniferyl alcohol, and cynarin, were found in the L-Sc3 vs. L-Sc2 group. In this study, it was observed that most phenolic acids tended to increase during the growth and development process. Specifically, 3'-methoxycrenatoside and 2-(3-β-D-glucopyranosyloxy-4-hydroxyphenyl) ethanol-1-O-β-D-glucopyranoside reached their maximum levels in the L-Sc3 stage.

One hundred forty-three differential alkaloids were identified, among which 32 alkaloids were identified as differentially abundant metabolites, including 11 alkaloids, 9 phenols, 4 polypeptides, 4 pyridine alkaloids, 1 benzylphenylethylamine alkaloid, 1 piperidine alkaloid, 1 piperidine alkaloid, and one quinorisidine alkaloid (Fig. 4C). Four unique alkaloids, namely, 4-hydroxy-3-methoxy-β-phenethylamine, diethanolamine, indole-5-carboxylic acid, and cis-Moschamine, were detected in the L-Sc1 vs. L-Sc2 comparison group. In the L-Sc1 vs. L-Sc3 group, 13 unique alkaloids, including gramine, isoquinoline, trigonelline, vasicine, and A-hydroxyquinoline, were identified. Additionally, 2 unique alkaloids, hydrocotarnine and sinapine, were found in the L-Sc3 vs. L-Sc2 group. In this study, the contents of most alkaloids tended to increase during the growth and development process. Specifically, salsoline A and salsolidine reached their maximum levels in the L-Sc2 stage.

Differentially abundant metabolite enrichment analysis at different stages

The enriched metabolites at different stages were determined through KEGG analysis, and the results are summarized and illustrated in Fig. 5. The greatest number of metabolites were included in the metabolic pathways (ko01100) and biosynthesis of secondary metabolites pathways (ko01110) categories. As shown in Fig. 5A, these DAMs were enriched mainly in metabolic pathways, biosynthesis of secondary metabolites, ABC transporters (ko02010), biosynthesis of cofactors (ko01240), biosynthesis of flavones aglycones I (MetMap110), and isorhamnetin O-glycosides biosynthesis (MetMap109) in L-Sc1 vs. L-Sc2. As shown in Fig. 5B, most DAMs involved in metabolic pathways, the biosynthesis of

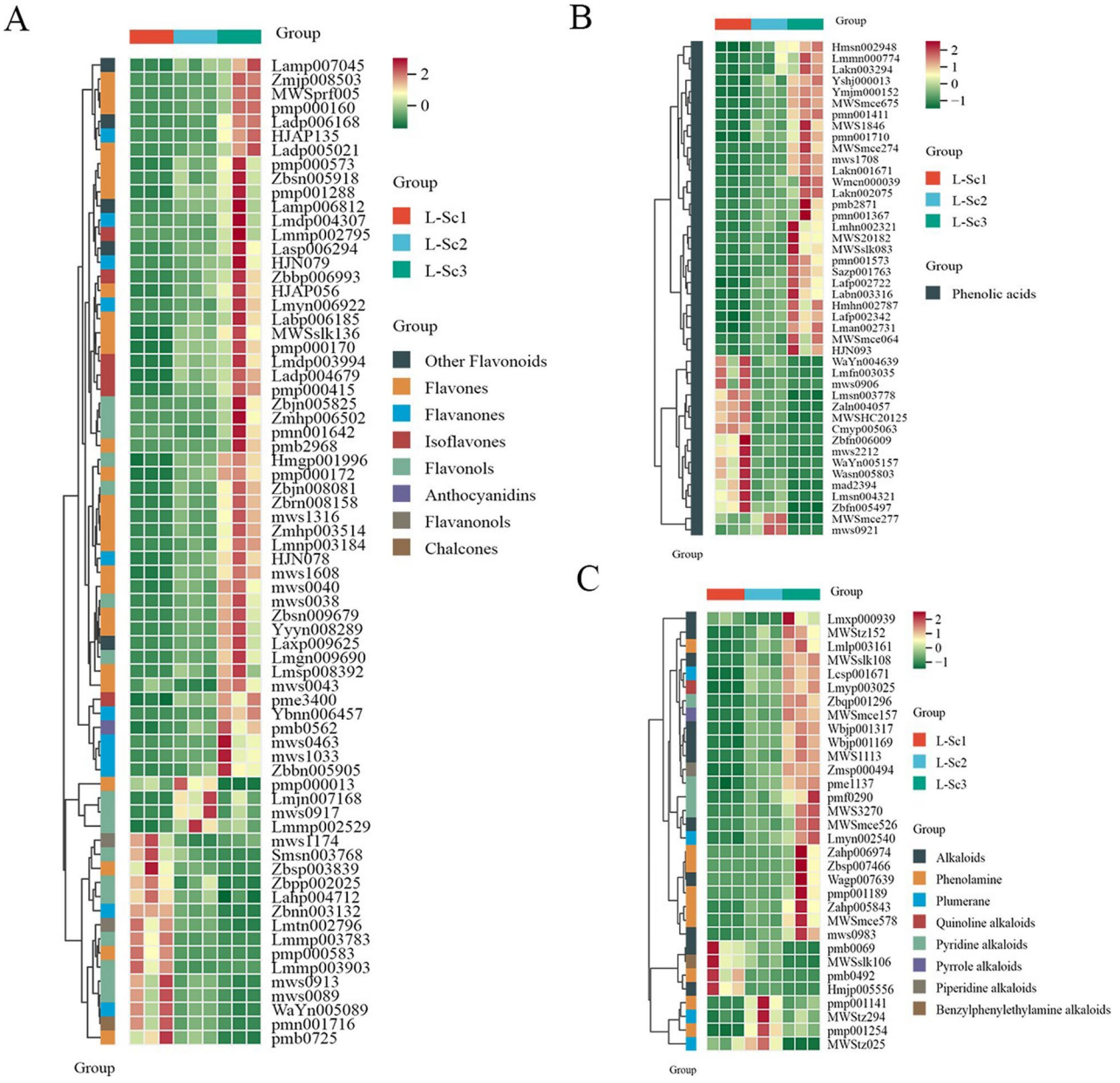

Fig. 4 (A) Heatmap of the flavonoid metabolites. **B** Heatmap of phenolic acid metabolism. **C** Heatmap of the differential alkaloids

secondary metabolites, ABC transporters, the biosynthesis of amino acids (ko01230), the biosynthesis of cofactors, and the biosynthesis of flavone aglycones I accumulated continuously with L-Sc1 vs. L-Sc3. Furthermore, the DAMs were enriched in metabolic pathways, biosynthesis of secondary metabolites, biosynthesis of amino acids, ABC transporters, flavonoid biosynthesis (ko00941), and biosynthesis of cofactors in L-Sc3 vs. L-Sc2 (Fig. 5C).

Transcript assembly of *S. collina* leaves at different stages

In order to investigate the gene expression profiles of the Salsola leaves at different stages, nine samples were subjected to RNA-seq (Table S8). A total of 404,443,482 high-quality reads with Q30 values higher than 92.9% were obtained after quality control, and 67,587 unigenes were subjected to *de novo* assembly using the Trinity software. The length was over 1000 bp for 38,658 unigenes (57.2%) and over 1500 bp for 28,669 (42.4%) unigenes. The average gene length and N50 length were 1648 and 2,413 bp, respectively. Functional unigene annotation was performed next, followed by mapping to the NCBI non-redundant (Nr) (49,309, 72.96%), Clusters of Orthologous Groups of proteins (KOG) (30,176, 44.65%), TrEMBL (48,376, 71.58%), A manually annotated and reviewed protein sequence database (Swiss-Prot) (36,458,

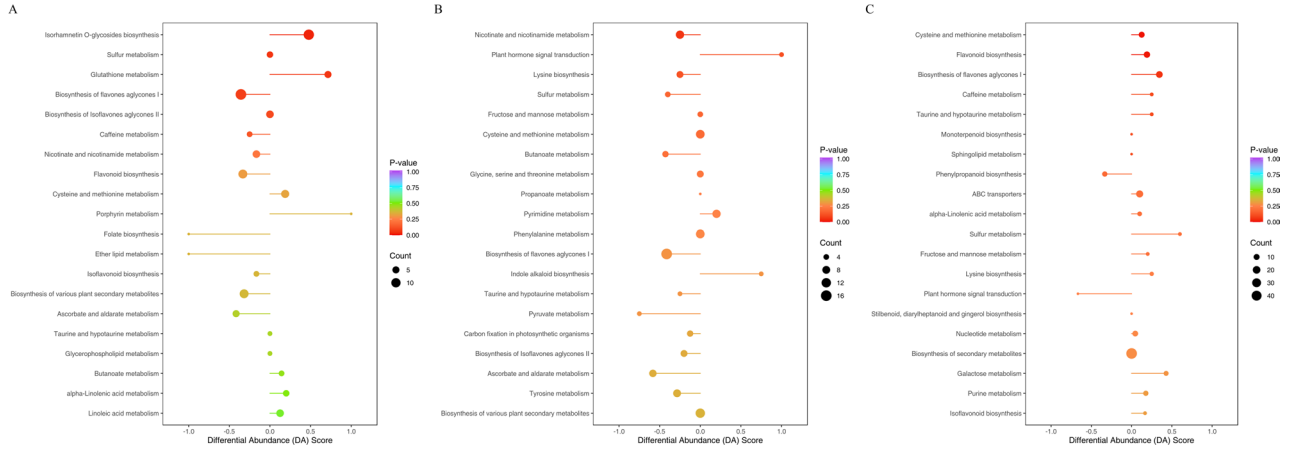

Fig. 5 KEGG pathway enrichment of the differentially expressed metabolites at different stages in Salsola leaves. **A** L-Sc1 vs. L-Sc2. **B** L-Sc1 vs. L-Sc3. **C** L-Sc3 vs. L-Sc2

53.94%), Kyoto Encyclopedia of Genes and Genomes (KEGG) (37,197, 55.04%), Protein family (Pfam) (38,594, 57.1%), and GO (42,628, 63.07%) databases.

Differential expression and functions of the genes involved in the leaves of *S. collina* at different stages

In order to analyze the gene expression patterns, the transcriptome data were centralized and standardized, and then analyzed using K-means clustering (Table S9). As shown in Fig. 6A, the genes were clustered into three subclasses. The number of 4,639 genes in subclass 1 exhibited the highest expression levels at the juvenile stage (L-Sc1). The 8,124 genes in subclass 2 presented the highest gene expression levels at the fruiting stage(L-Sc3). Furthermore, 3,437 genes in subclass 3 displayed maximal expression at the fruiting stage (L-Sc2). As shown in Fig. 6B, different numbers of DEGs among different stages were identified: L-Sc1 vs. L-Sc2 (4,688 DEGs: 1,656 up, 3,032 down), L-Sc1 vs. L-Sc3 (12,685 DEGs: 5,074 up, 7,611 down), L-Sc3 vs. L-Sc2 (10,338 DEGs: 5,533 up, 4,805 down). Analysis of the data from the three comparisons revealed 979 common DEGs, which are shown in the Venn diagram depicted in Fig. 6C.

In the GO analysis, 4,688 DEGs were revealed to be enriched in the comparison of L-Sc1 vs. L-Sc2 into 3 classes and 43 subclasses, 12,685 DEGs from the comparison of L-Sc1 vs. L-Sc3 were enriched into 3 classes and 45 subclasses, and 10,338 DEGs from the comparison of L-Sc3 vs. L-Sc2 were enriched into 3 classes and 44 subclasses. Among these DEGs, 2,149 (857 upregulated and 1,292 downregulated), 5,572 (2,366 upregulated and 3,206 downregulated), and 4,509 (2,425 upregulated and 2,084 downregulated) DEGs in the adjacent groups were annotated with GO terms related to "metabolic process". The analysis of the secondary metabolite biosynthesis, terpenoid metabolism, phenylpropanoid metabolism, alkaloid metabolic processes, and flavonoid metabolism at different stages revealed significant differences in the genes (Fig. 7A). Moreover, in the KEGG pathway enrichment analysis, the most enriched DEGs were associated with metabolic pathways, biosynthesis of secondary metabolites, plant hormone signal transduction, phenylpropanoid biosynthesis, and flavonoid biosynthesis (Fig. 7B).

Integrated analysis of transcriptomics and metabolomics

Integrated transcriptomics and metabolomics analyses enable a more comprehensive understanding of the gene regulatory mechanisms governing metabolic processes. Therefore, to determine the intricate relationships between genes and metabolites in the present study, the differentially expressed genes and differentially accumulated metabolites from each comparison group were mapped to the Kyoto Encyclopedia of Genes and Genomes pathways. As shown in Fig. 8A and Table S10, 1,805 DEGs and 172 DAMs could be mapped to 68 KEGG pathways, among which 16 pathways were significantly enriched in L-Sc1 vs. L-Sc2, including phenylpropanoid biosynthesis (ko00940), biosynthesis of secondary metabolites (ko01110), flavonoid biosynthesis (ko00941), metabolic pathways (ko01100), and isoquinoline alkaloid biosynthesis (ko00950). In L-Sc1 vs. L-Sc3, 4,845 DEGs and 236 DAMs were mapped to 87 KEGG pathways, with 32 pathways significantly enriched (Fig. 8B and Table S11), such as the biosynthesis of secondary metabolites, phenylpropanoid biosynthesis, flavonoid biosynthesis, metabolic pathways, and plant hormone signal transduction (ko04075). Figure 8C and Table S12 shows the 3,878 DEGs and 158 DAMs mapped to 74 KEGG pathways in L-Sc3 vs. L-Sc2, among which the biosynthesis of secondary metabolites, metabolic pathways, phenylpropanoid biosynthesis, biosynthesis of various plant secondary metabolites (ko00999), pentose and glucuronate interconversions (ko00040), and flavonoid biosynthesis were

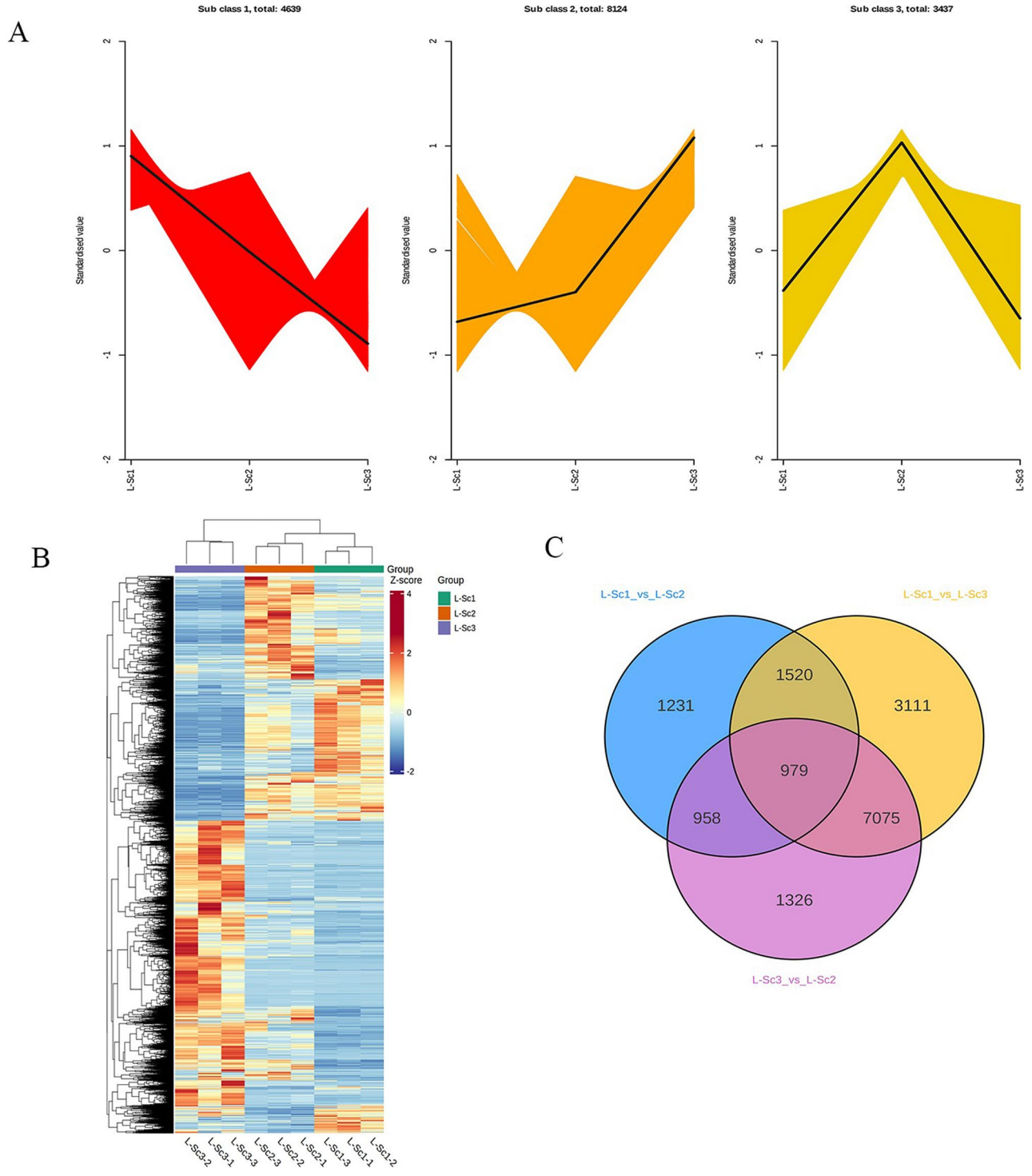

Fig. 6 Analysis of the differentially expressed genes (DEGs) in the leaves of *Salsola* across different developmental stages. **A** K-means clustering analysis of the gene expression patterns in *Salsola* leaves. **B** Cluster heatmap of the DEGs between *Salsola* leaves. **C** Venn diagram of the DEGs in the L-Sc1 vs. L-Sc2, L-Sc1 vs. L-Sc3, and L-Sc3 vs. L-Sc2 comparisons

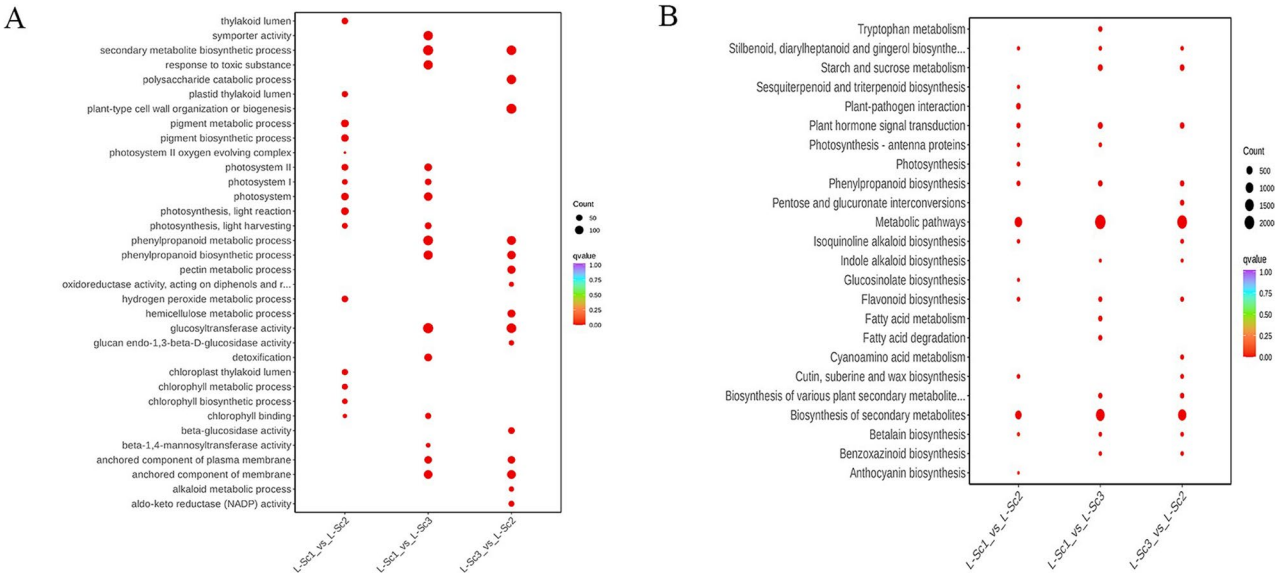

Fig. 7 (**A**) Enriched GO analysis of the DEGs between different stages. **B** Enriched KEGG pathways of the DEGs between different stages

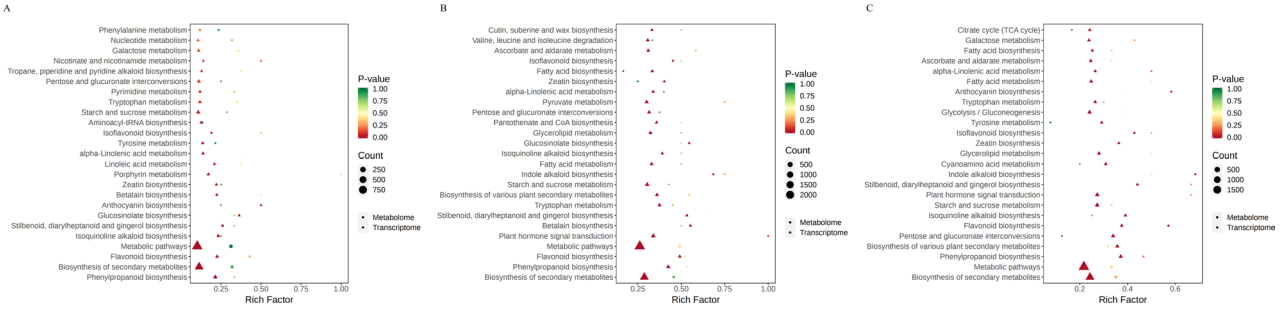

Fig. 8 KEGG pathway enrichment of the DEGs and DAMs in the different stages of *Salsola* leaf development. **A** L-Sc1 vs. L-Sc2. **B** L-Sc1 vs. L-Sc3. **C** L-Sc3 vs. L-Sc2

enriched. Overall, among these three comparison groups, "phenylpropanoid biosynthesis" and "flavonoid biosynthesis" presented high enrichment levels, indicating that flavonoid biosynthesis is crucial for its development of *S. collina*.

Dynamic regulation of the key gene families involved in flavonoid biosynthesis during different stages in *S. collina* leaves

The results of the KEGG enrichment analysis of the DEGs and DAMs revealed that phenylpropanoid biosynthesis and flavonoid biosynthesis were significantly enriched in *S. collina*. Therefore, changes in the flavonoid biosynthesis-related genes and metabolites were studied further (Fig. 9). In this study, a total of 258 DEGs were detected, including 69 differentially expressed flavonoid structural genes (1 *PAL*, 4 *C4H*, 12 *4CL*, 14 *CHS*, 4 *CHI*, 6 *F3H*, 1 *F3'5'H*, 6 *FM3MO*, 8 *DFR*, 6 *FLS*, and one *ANS* gene, among others). As shown in Fig. 9A, the relatively high expression of *C4H* and *4CL* was detected in L-Sc2, whereas *PAL*, *CHS*, *CHI*, *F3H*, *FLS*, and *ANS* gradually increased. As *S. collina* leaves developed, the downstream regulatory genes *FM3MO*, *F3H*, *ANS*, and *FLS* were highly expressed in L-Sc3, which promoted the maximum accumulation of downstream flavonoids, such as those in this stage.

As shown in Figs. 9B and C and 26 DAMs involved in phenylpropanoid biosynthesis and flavonoid biosynthesis were detected. Fifteen DAMs were identified in the flavonoid biosynthetic pathway, including 5 flavanones, 2 chalcones, 2 flavanonols, 2 flavones, 2 phenolic acids, 1 flavonol, and one flavonol. Naringenin chalcone and naringenin are pivotal metabolites in flavonoid synthesis and are accumulated at relatively high levels in L-Sc2. Kaempferol, myricetin, and lutein gradually increased in levels, with the greatest increase noted in L-Sc3. Overall, the expression trends of most of the DEGs and DAMs were essentially consistent, with upregulation during leaf development.

In order to verify the accuracy of the transcriptome analysis results, 6 flavonoid structural genes were randomly selected and subjected to qRT-PCR validation.

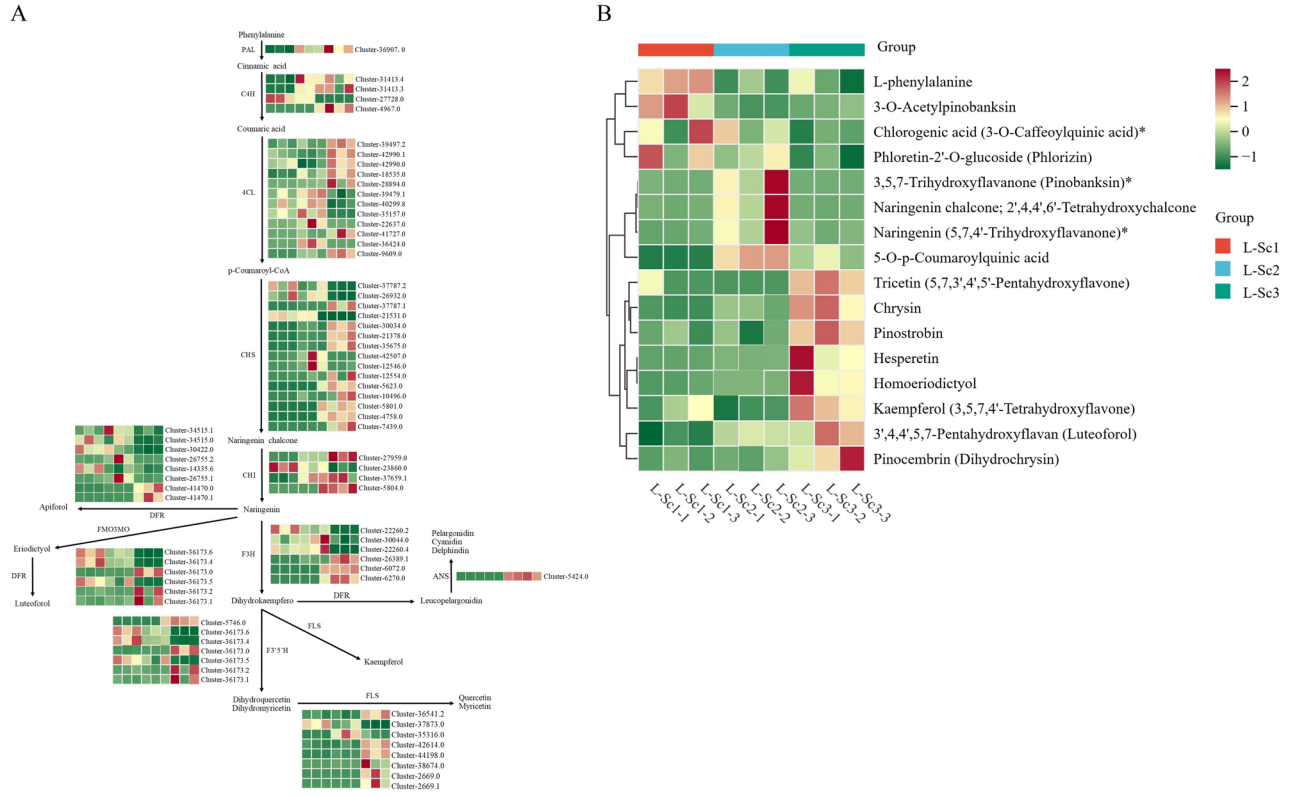

Fig. 9 **A** Flavonoid biosynthesis pathway in *Salsola* leaves. **B** Heatmap of the flavonoid metabolites involved in phenylpropanoid biosynthesis and flavonoid biosynthesis. The heatmaps are drawn based on the FPKM values from the transcriptome datasets. The columns and rows in the heatmap represent the samples and genes, respectively, and the color scale indicates fold changes (log10) in gene expression

The qRT-PCR analysis of all 6 genes revealed the same expression trends as those noted for the RNA-Seq data. Pearson's correlation coefficients further indicated that the digital transcript abundance measurements of most genes were highly correlated with the qRT-PCR data. These results confirmed the reliability of the RNA-Seq data (Fig. 10).

Discussion

S. collina is a widely recognized medicinal and edible plant. Numerous studies have identified the chemical constituents of this species, and most of these studies have focused on its pharmacological activities [1, 4, 7–10]. Only a few systematic investigations have been conducted to determine the dynamic evolution patterns of metabolites and their regulatory mechanisms throughout the growth cycle. An integrated analytical framework combining untargeted metabolomics and RNA sequencing was employed in this study to elucidate the metabolic landscape and transcriptome alterations in developing *S. collina* foliage. A total of 1,820 metabolites were successfully identified, covering multiple major categories, such as flavonoids, phenolic acids, alkaloids, lipids, amino acids, and their derivatives. The results of this study have greatly improved the understanding of the chemical composition of *S. collina*.

In a previous study, 131 DAMs of flavonoids were detected from the shoots and roots of *S. collina*, and most of these flavonoids had relatively high concentrations in the shoots [13]. The present study revealed substantial alterations in both flavonoid biosynthesis-related gene expression and metabolite accumulation throughout leaf development in *S. collina*. In *S. collina* foliage, 252 differential flavonoid metabolites were identified in this study, constituting 23.85% of all the identified metabolites. A total of 258 DEGs and 26 DAMs were identified in the three growth stages using metabolomics and transcriptomics data. In the metabolomics analysis, phenylalanine was revealed to be more highly expressed in the juveniles than in the flowers and fruits, naringenin chalcone and naringenin accumulated at relatively high levels during flowering, and kaempferol, myricetin, luteolin, and lutein were expressed at their respective maximum levels during fruiting. The C4H and 4CL genes were expressed at relatively high levels during flowering, and the expression levels of most CHS, F3H, FLS, and ANR genes were relatively high during fruiting. The co-expression of these genes likely contributes to flavonoid biosynthesis, which

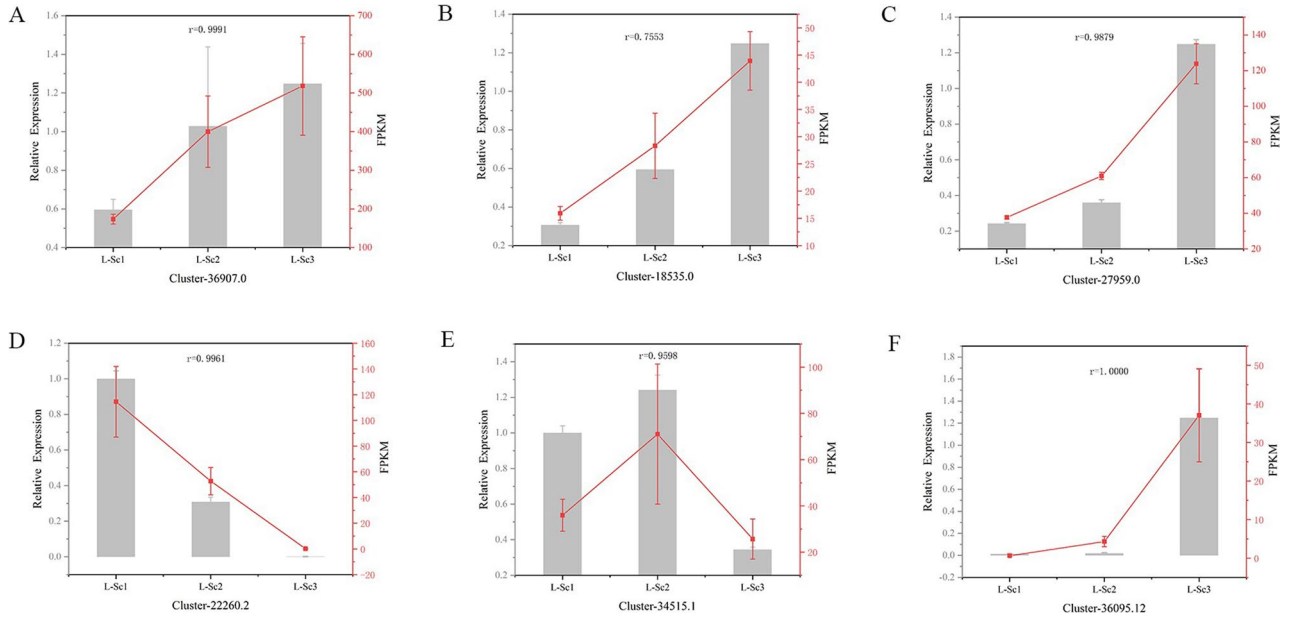

Fig. 10 Expression analysis of the flavonoid structural genes in the leaves of Salsola at different stages. **A***PAL*, (**B**) *4CL*, (**C**) *CHI*, (**D**) *F3H*, (**E**) *DFR*, (**F**) *CCR*

explains the increased accumulation of these genes in *S. collina* leaves.

Flavonoids, as key plant secondary metabolites, play indispensable roles in regulating plant growth and development, as well as in mediating plant responses to biotic and abiotic stresses [30, 31]. Flavonoid biosynthesis is initiated at the convergence of the shikimate pathway and the acetate-derived polyketide pathway [32]. Phenylalanine is a key precursor for flavonoid biosynthesis, which is converted to *p*-coumaroyl-CoA under the catalysis of PAL, C4H, and 4CL [33]. Further, p-Coumaroyl CoA and malonyl CoA condense and isomerize through CHS to form naringenin chalcone, which is rapidly cyclized to naringenin by the chalcone isomerase CHI [34]. Naringenin is the key metabolite in flavonoid synthesis, which drives the structural similarity among flavonoids [35]. In this study, the genes encoding CHS and CHI were revealed to be significantly associated with downstream flavonoid compounds. During leaf maturation, the transcriptional activity of CHS and CHI increased progressively, concomitant with the increased accumulation of naringenin chalcone and naringenin.

In addition, naringenin can be converted into dihydrokaempferol by F3H and subsequently transformed into dihydroquercetin and dihydromyricetin by F3′H and F3′5′H, respectively. FLS subsequently catalyzes the conversion of these dihydroflavonol intermediates into their corresponding flavonol end products, including kaempferol, quercetin, and myricetin [36]. In this study, the analysis of transcriptomics and metabolomics data revealed that three genes, F3'H, F3'5'H, and FLS, presented significantly upregulated expression across growth. Specifically, these three genes presented markedly increased expression levels at the fruiting stage, while their catalytic products, namely, kaempferol, myricetin, and lutein, also presented increased expression during this stage. A previous study reported that F3'H and F3'5'H are the key enzymes involved in flavonoid synthesis, affecting the formation of dihydroxylated and trihydroxylated catechins in *Camellia sinensis* [37].

Integrated transcriptomics and metabolomics analyses have been widely employed to reveal the variation patterns of flavonoids during the growth and development of different plant species. Compared with leaf buds, mature jujube leaves contain abundant flavonoids and phenolic acids, conferring high antioxidant potential to the leaves [38]. Most flavonoids accumulate in the early fruiting stage, and their levels decrease at the following developmental stages in *Citrus sinensis* [39]. Driven by the high expression of the CHS and CHI genes, *Dendrobium huoshanense* stems presented a significant increase in the total flavonoids in the 3rd year. This process generates key precursors, such as naringin, which in turn activate the downstream FLS gene, resulting in the explosive accumulation of the final products, such as quercetin [40]. In this study, the total flavonoid content at the flowering stage was 8.944 mg/g, which was significantly greater than that at the juvenile and fruiting stages. These results indicate a correlation between flavonoid accumulation and the expression of related key genes during the growth of *S. collina* leaves. Notably, genes are inextricably linked to metabolites, and their expression typically correlates consistently with the downstream metabolite levels, while the differential expression of key genes directly

drives the accumulation or reduction of the metabolites during plant growth. Thus, integrated metabolomics and transcriptomics analyses serve as a powerful approach to identify the core genes and metabolites involved in biosynthetic pathways.

Conclusion

In this study, 1,820 metabolites were identified from *S. collina* leaves, and 1,125 metabolites that differed significantly during the development stages were identified. Flavonoids, phenolic acids, and alkaloids were the major DAMs. Moreover, the DEGs and MAMs involved in flavonoid biosynthesis in *S. collina* foliage were analyzed, and it was determined that the increased expression of several key genes promoted the accumulation of downstream flavonoid substances. Key chemical components, including total flavonoids, polyphenols, and alkaloids, were quantitatively analyzed. The maximum values of the key chemical components occurred in the flowering stage. These results improve the understanding of the chemical components and medicinal value of *S. collina* leaves and provide theoretical support for the development of *S. collina* foliage as a functional food.

Abbreviations

UPLC-MS/MS	Ultra Performance Liquid Chromatography-Tandem Mass Spectrometry
LC-MS	Liquid chromatography-mass spectrometry
LIT	Linear ion trap
QQQ	Triple quadrupole
DAMs	Differentially accumulated metabolites
MRM	Multiple reaction monitoring
RT	Retention time
PCA	Principal component analysis
OPLS-DA	Orthogonal partial least squares-discriminant analysis
VIP	Variable importance in project
FPKM	Fragments Per Kilobase of transcript per Million fragments mapped
DEGs	Differentially expressed genes
NCBI	National Center for Biotechnology Information
Nr	NCBI non-redundant protein sequences
TrEMBL	A variety of new documentation files and the creation of TrEMBL, a computer annotated supplement to SWISS-PROT
Pfam	Protein family
KOG	Clusters of Orthologous Groups of proteins
KO	KEGG Ortholog database
GO	Gene Ontology
Swiss-Prot	A manually annotated and reviewed protein sequence database
KEGG	Kyoto Encyclopedia of Genes and Genomes
FC	Fold change
FDR	False discovery rate
qRT-PCR	Quantitative real-time PCR
PAL	Phe ammonia-lyase
C4H	Cinnamic acid 4-hydroxylase
4CL	4-Coumaroyl CoA ligase
CHS	Chalcone synthase
CHI	Chalcone isomerase
F3H	Flavanone 3-hydroxylase
FM3MO	Flavonoid 3′-monooxygenase
F3'5'H	Flavanone 3′-5′-hydroxylase
DFR	Dihydroflavonol 4-reductase
ANS	Anthocyanidin synthase

Supplementary Information

The online version contains supplementary material available at https://doi.org/10.1186/s12870-026-08856-5.

Supplementary Material 1.

Supplementary Material 2.

Acknowledgements

Not applicable.

Authors' contributions

Y.C. conducted most of the experiments. W.B., J.H. and W.W. performed total flavonoid, polyphenol, and alkaloid contents analysis. S.L., S.Z., M.W., Y.F. and Y.M. participated in Metabolite profiling and RNA-Seq analysis. H.Y. initiated the project. Y.C. and H.Y. designed and supervised the study. Y.C., S.L. and H.Y. analyzed the data and wrote the manuscript. All authors have read and approved the manuscript.

Funding

This work was supported by the Key Science and Technology Program of Henan Province (project No. 242102310580 and 252102230108), and Key Scientific Research Projects of Universities in Henan Province (project No. 26A220005 and 26B180006).

Data availability

All data analyzed during this study are included in this published article and its supplementary information files. The transcriptome datasets are available in the NCBI Sequence Read Archive database (accession number, SRR36930806- SRR36930814).

Declarations

Ethics approval and consent to participate

Not applicable.

Consent for publication

Not applicable.

Competing interests

The authors declare no competing interests.

Received: 12 December 2025 / Accepted: 22 April 2026
Published online: 29 April 2026

References

1. Eldehna 1ENMH, Abourehab WM, Abdel Bar MA. The old world *salsola* as a source of valuable secondary metabolites endowed with diverse pharmacological activities: a review. J Enzyme Inhib Med Chem. 2022;37:1.
2. Kong X. Chenopodiaceae. Flora Repubulicae Popularis Sinicae; Editorial Committee of Chinese Flora. Volume 25. Beijing,China: Ed.; Science; 1979. p. 176.
3. Compilation group of national compilation of Chinese herbal medicine. National compilation of Chinese herbal medicine; people's medical publishing house: Beijing, China. 1975;(2):796–7.
4. Wang S, Yan M, Guo Y, Sun R, Jin H, Gong Y. In vivo and in vitro effects of *Salsola collina* on gastrointestinal motility in rats. Iran J Basic Med Sci. 2020;23(3):383.
5. Zhao X, Wang H, Zhang Z, Jin H, Gong Y. Effects of ethyl acetate extract of *Salsola collina* on brain-gut peptides and interstitial cells of gastric Cajal in rats with diabetic gastroparesis. Iran J Basic Med Sci. 2020;23:1218–24.
6. Zhao XL, Yuan W, Li ZZ, Jin H, Gong YL. *Salsola collina* ethyl acetate extract alleviates diabetic gastroparesis possiblythrough oxidative stress inhibition. In IOP Conference Series: Earth and Environmental Science; IOP Publishing Ltd.: Bristol, UK. 2020;559:012021.
7. Wang J, Liu W, Huang Y, Wang G, Guo X, Shi, Shi D, Sun T, Xiao C, Zhang C, Jiang B, Guo Y, Li JA. Senomorphlytic Three-Drug Combination Discovered

in *Salsola collina* for Delaying Aging Phenotypes and Extending Healthspan. Adv Sci. 2024;11(36):2401862.
8. Zhao YX, Ding XB. Studies on the alkaloids from *Salsola collina* Pall. Acta Pharm Sin. 2004;39:598–600.
9. Xiang Y, Li YB, Zhang J, Li P, Yao YZ. Studies on chemical constituents of *Salsola collina*. China J Chin Mater Med. 2007;32:409-413.9.
10. Jin YS, Du JL, Yang Y, Jin L, Song Y, Zhang W, Chen HS. Chemical and biologically active constituents of *Salsola collina*. Chem Nat Compd. 2011;47:257–60.
11. Wang XJ, Zhao YX, Jia XH, Ding XB. Studies on the chemical constituents of *Salsola collina*. J Chin Med Mater. 2011;34:230–1.
12. Ghorab H, Khettaf A, Lehbili M, Kabouche A, Magid AA, Harakat D, Voutquenne-Nazabadioko L, Kabouche Z. A new cardenolide and other compounds from *Salsola tetragona*. Nat Prod Commun. 2017;12:1934578X1701200102.
13. Li S, Chen Y, Duan Y, Zhao Y, Zhang D, Zang L, Ya H. Widely targeted metabolomics analysis of different parts of *Salsola collina* pall. Molecules. 2021;26(4):1126.
14. Li Y, Kong D, Fu Y, Sussman MR, Wu H. The effect of developmental and environmental factors on secondary metabolites in medicinal plants. Plant Physiol Biochem. 2020;148:80–9.
15. Jia YS, Zhang XJ, Tan NH. Research progress on temporal-spatial characteristics of chemical components in traditional Chinese medicinal materials. Chinese Traditional and Herbal Drugs. 2024;55(24):8580–858816.
16. Li Y, Wu H. The Research Progress of the Correlation Between Growth Development and Dynamic Accumulation of the Effective Components in Medicinal Plants. Chin Bull Bot. 2018;53(3):293–304.
17. Kou YN, Zhang X, Kong FK, Dong HJ, Yang J, Wang WH, Kong DZ, Yang B. Content of secondary metabolites and antioxidant activities of *Lonicera japonica* flowers at different developmental stages from Shandong province. China J Chin Materia Med. 2024;49(10):2654–65.
18. Liu C, Yan F, Bi J, Li Z, Bao H, Song M. Hepatoprotective Effect of C. versicolor Fruiting Body Water Extracts at Different Developmental Stages. Acta Edulis Fungi. 2021;28(3):122–8.
19. Chen W, Gong L, Guo Z, Wang W, Zhang H, Liu X, Luo JA. Novel Integrated Method for Large-Scale Detection, Identification, and Quantification of Widely Targeted Metabolites: Application in the Study of Rice Metabolomics. Mol Plant. 2013;6(6):1769–80.
20. Wang A, Li R, Ren L, Gao X, Zhang Y, Ma Z, Ma D, Luo Y. A comparative metabolomics study of flavonoids in sweet potato with dierent flesh colors (*Ipomoea batatas* (L.) Lam). Food Chem. 2018;260:124–34.
21. Worley B, Powers R. PCA as a practical indicator of OPLS-DA model reliability. Curr Metabolomics. 2016;4(2):97–103.
22. Jordon-Thaden IE, Chanderbali AS, Gitzendanner MA, Soltis DE. Modified CTAB and TRIzol Protocols Improve RNA Extraction from Chemically Complex Embryophyta. Applications in Plant Sciences. 2015.
23. Grabherr MG, Haas BJ, Yassour M, Levin JZ, Thompson DA, Amit I, Full-length transcriptome assembly from RNA-Seq data without a reference genome. Nature Biotechnology., Huber MI, Anders W et al. S. Moderated estimation of fold change and dispersion for RNA-seq data with DESeq2. Genome biology. 2014;15(12):550.
24. Varet H, Brillet-Guéguen L, Coppée J-Y, Dillies M-A, SARTools. A DESeq2- and EdgeR-based r pipeline for comprehensive differential analysis of RNA-seq data. PLoS ONE. 2016;11:e0157022.
25. Livak KJ, Schmittgen TD. Analysis of relative gene expression data using real-time quantitative PCR and the 2 – ΔΔCT method. Methods. 2001;25(4):402–8.
26. Chen Y, Meng G, Liu X, Ya H, Li S. Analysis of Transcriptome Characteristics of Different Parts of *Salsola collina* Pall. Mol Plant Breed. 2022;20(16):5319–31.
27. Lu X, Chen G, Ma L, Zhang C, Yan H, Bao J, Nai G, Wang W, Chen B, Ma S, Li S. Integrated transcriptome and metabolome analysis reveals antioxidant machinery in grapevine exposed to salt and alkali stress. Physiol Plant. 2023;175(3):e13950.
28. Wang Y, Gao S, He X, Li Y, Zhang Y, Chen W. Response of total phenols, flavonoids, minerals, and amino acids of four edible fern species to four shading treatments. PeerJ. 2020;8:e8354.
29. Feng H, Zhao Y, Wang XY, Hao L. Optimization of purification process of total alkaloid extract of berberis dictyophylla cortex by macroporous resin and investigation of its quality standard. Chin J Experimental Traditional Med Formulae. 2019;25(16):97–103.
30. Liu W, Feng Y, Yu S, Fan Z, Li X, Li J, Yin H. The flavonoid biosynthesis network in plants. Int J Mol Sci. 2021;22(23):12824.
31. Shen N, Wang T, Gan Q, Liu S, Wang L, Jin B. Plant flavonoids: Classification, distribution, biosynthesis, and antioxidant activity. Food Chem. 2022;383:132531.
32. Ku YS, Ng MS, Cheng SS, Lo AWY, Xiao Z, Shin TS, Chung G, Lam H-M. Understanding the Composition, Biosynthesis, Accumulation and Transport of Flavonoids in Crops for the Promotion of Crops as Healthy Sources of Flavonoids for Human Consumption. Nutrients. 2020;12:1717.
33. Tohge T, de Souza LP, Fernie AR. Current understanding of the pathways of flavonoid biosynthesis in model and crop plants. J Exp Bot. 2017;68(15):4013–28.
34. Liu CY, Yan F, Bi JF, Li ZJ, Bao HY, Song MJ. Hepatoprotective Effect of *C.versicolor* Fruiting Body Water Extracts at Different Developmental Stages. Acta Edulis Fungi. 2021;28(3):122–8.
35. Kim JI, Hidalgo-Shrestha C, Bonawitz ND, Franke RB, Chapple C. Spatio-temporal control of phenylpropanoid biosynthesis by inducible complementation of a cinnamate 4-hydroxylase mutant. J Exp Bot. 2021;2021(728):3061–73.
36. Yonekura-Sakakibara K, Higashi Y, Nakabayashi R. The origin and evolution of plant flavonoid metabolism. Front Plant Sci. 2019;10:943.
37. Wei K, Wang L, Zhang C, Wu L, Li H, Zhang F, Cheng H. Transcriptome analysis reveals key flavonoid 3′-hydroxylase and flavonoid 3′, 5′-hydroxylase genes in affecting the ratio of dihydroxylated to trihydroxylated catechins in *Camellia sinensis*. PLoS ONE. 2015;10(9):e0137925.
38. Li S, Deng B, Tian S, Guo M, Liu H, Zhao X. Metabolic and transcriptomic analyses reveal different metabolite biosynthesis profiles between leaf buds and mature leaves in *Ziziphus jujuba* mill. Food Chem. 2021;347:129005.
39. Xu J, Yan J, Li W, Wang Q, Wang C, Guo J, Geng D, Guan Q, Ma F. Integrative Analyses of Widely Targeted Metabolic Profiling and Transcriptome Data Reveals Molecular Insight into Metabolomic Variations during Apple (*Malus domestica*) Fruit Development and Ripening. Int J Mol Sci. 2020;21:4797.
40. Yuan Y, Zuo J, Zhang H, Li R, Yu M, Liu S. Integration of transcriptome and metabolome provides new insights to flavonoids biosynthesis in *Dendrobium huoshanense*. Front Plant Sci. 2022;13:850090.

Publisher's note